DOI: 10.11830/ISSN.1000-5013.201801006

New Discontinuity Indicator for DG Method Using Local Variation

HUANG Rixin[1], TAN Yonghua[2], WU Baoyuan[1], LI Guangxi[1]

(1. Xi'an Aerospace Propulsion Institute, Xi'an 710100, China;
2. Academy of Aerospace Propulsion Technology, Xi'an 710100, China)

Abstract: Inspired by the concept of total variation in the total variation bounded (TVB) methods, a similar concept of local variation for discontinuous Galerkin (DG) method was presented. Based on the local variation, a rigorous bounding procedure for error evaluation in the Soblev's space was conducted, and then a new type of discontinuity indicator was developed to detect the locations of discontinuities such as shock and contact *et al*. Compared with the detectors in the finite volume method, the new indicator is completely local within an element and does not rely on any information from neighboring elements. As a result, the indicator features intrinsic characteristics of the finite element method and is very simple to implement. The typical numerical examples show a good performance of the newly constructed indicator and it becomes a proper candidate for detecting tasks of DG applications.

Keywords: discontinuity indicator; discontinuous Galerkin method; local variation; Gegenbauer reconstruction; Euler equation

CLC Number: U 491.17 **Document Code**: A **Article Number**: 1000-5013(2018)04-0520-06

应用 DG 方法的新型局部变差间断监测器

黄日鑫[1], 谭永华[2], 吴宝元[1], 李光熙[1]

(1. 西安航天动力研究所, 陕西 西安 710100;
2. 航天推进技术研究院, 陕西 西安 710100)

摘要: 受到总变差有界(TVB)方法中总变差概念的启示,提出适用于间断伽辽金(DG)方法的局部变差概念.在此基础上,对 Soblev 空间中的误差估计进行严格的界定,建立一种能够准确甄别激波与接触间断等间断位置的新型识别器.研究结果表明:与有限体积方法中的间断监测器相比,该新型识别器完全基于单元局部,不需要依靠相邻单元的任何信息,具有典型的有限元方法的固有属性,更容易在算法上实现.通过典型的数值算例对该识别器进行验证,结果表明:该识别器非常出色地实现对间断位置的识别,可用于间断元方法的间断位置监测.

关键词: 间断监测器; 间断伽辽金方法; 局部变差; 盖根鲍尔重构; 欧拉方程

Though labeled as a promising high order method in extensive applications, the discontinuous Galerkin (DG) method suffers from Gibbs phenomenon and induces nonlinear instabilities in the neighborhood of strong discontinuities, and consequently risks a breakdown of the solution that is under resolved severely. The spurious numerical oscillations of the Gibbs phenomenon are introduced intrinsically by high-order of accuracy itself; owing to the theory it proclaims strictly no monotone

收稿日期: 2017-03-29
通信作者: 谭永华(1963-),研究员,博士,主要从事航空宇航推进理论及工程的研究. E-mail:tanyhcasc@163.com.
基金项目: 国家自然科学基金资助项目(11702205)

schemes exist beyond first order accuracy. However, this does not mean a final argument of the use of high-order methods[1-2] for solutions with discontinuities, but triggers several strategies to eliminate the unpleasant oscillations.

A popular strategy is that marks trouble cell using a discontinuity indicator first, and then employs an oscillation eliminated technique to suppress wrinkles. The discontinuity indicator is also called a shock detector in finite volume methods, and most commonly used are detectors based on total variation bounded (TVB) limiters[3], KXRCF type detectors[4], shock detectors derived from Mac Cormack viscosity correction[5], and detectors based on shock characteristics[6] *et al*. Hao, *et al*[7] have made a comprehensive research on these detectors, and showed that the detectors based on shock characteristics are better than KXRCF ones, but the latter have wider applications. The results from Zhong, *et al*[8] showed a good performance of the TVB based detectors for structured grids. Zhu, *et al*[9] used the KXRCF detectors for unstructured grids, and marked the oscillatory regions nearby the shocks reasonably. Considering the jumps on the common interfaces between two neighboring elements. Zhang, *et al*[10] constructed a new discontinuity detector and eliminated the oscillations effectively.

As the DG methods allow discontinuities along the shared interfaces between two elements, there would be no oscillations if these discontinuities rightly stand on the interfaces coincidently. However, this coincident scenario is actually very hard to fulfill. And the discontinuities always run through the elements, which undoubtedly burdens the detecting task. The detectors described above paid more attention to the element interfaces, which is just fine for the finite volume method, because the only elemental averages cannot carry more supports and resorting to other elements via interfaces is obviously necessary. But for the discontinuous element methods, such as DG, it is absolutely straightforward to dig deep for full information inside a single element. And this is also exactly what we are engaged in this paper, therefore a new indicator of discontinuities for DG method is presented based on local variation referring to the concepts of TVB method. To distinguish from the above detectors, we call it an indicator for a much sharper capture capability for discontinuities.

1　Discontinuous Galerkin Method

Consider the hyperbolic conservation laws of the form $q_t+f_x(q)=0$, $q=q^0$, $q=q^b$. q is the conservative variable, and f is the corresponding flux. x is the Cartesian coordinates in physical domain Ω. The superscript 0 and b represent initial and boundary conditions respectively. By approximating the domain Ω with a collection of geometry conforming elements Ω_k as $\Omega \approx \sum_{k=1}^{K}\Omega_k$, where K is the number of elements. Then express the local solution on an element in the nodal form through the associated Lagrange polynomial $l_j(x)$, as $x \in \Omega_k: q_k = \sum_{i=1}^{n_p} q_k(x_i) l_i(x)$. Where n_p is the number of nodes. Assume N is the top degree of interpolation polynomials, as $n_p=(N+d,N)$.

Integrating the system over Ω_k, preferring the space of weighted or test functions to be the same with the base functions, we form the Galerkin formula. By performing integration by parts, or using the divergence theorem twice, we obtain

$$(l_j, q_t)_{\Omega_k} + (l_j, f_x)_{\Omega_k} + \langle l_j, (f_n^* - f_n)\rangle_{\partial\Omega_k} = 0,$$

as the strong form of DG discretization. $(\cdot)$ and $\langle\cdot\rangle$ denote the volume and surface inner products in L^2 space respectively. The superscript "$*$" indicates the numerical flux determined by the exact Riemann solver or an approximate Riemann solver. $f_n=\boldsymbol{f}\cdot\boldsymbol{n}$ is the outward normal component of the flux at the boundary. Though introducing remarkable aliasing errors, we prefer an interpolation of $\boldsymbol{f}$

in the same manner as q. Then define the mass matrix and the stiff matrix of the form are $\boldsymbol{M}_{i,j}=(l_i, l_j)$, $\boldsymbol{S}_{i,j}=(l_i, l_{j,x})$.

Note that, the modal form of the approximation of the solution is utilized to ease the computations of these matrices during further implementations, and then after several manipulations of matrix and vector, we finally get the semi-discrete form is $\frac{\mathrm{d}q}{\mathrm{d}t}=R(q)$.

A fourth order explicit SSP-RK method[11-12] is used here for time marching.

2 Indicator

For nonlinear problems with smooth solutions, the DG method has the following error estimates[13], as $\| q-q_h \|_{0,1}\leqslant Ch^{N+1}|u|_{N+1,1}$. Where a regular grid, $h=\max(h_k)$, is used. q and q_h are exact and numerical solutions respectively. C is a constant depending on q, N, and time, but not on h. All errors are measured in Soblev′s space. When written locally, the error estimates of a local element with smooth solutions must be bounded in the same manner as the above equation. For DG method, define local variation for an element as $\mathrm{LV}=\| q_h-\bar{q} \|_{0,1}$, then we can obtain the following error bounds

$$\mathrm{LV}\leqslant \| q_h-q \|_{0,1}+\| q-\bar{q} \|_{0,1}\leqslant Ch\,|\,q\,|_{1,1}+O(h^{N+1}), \tag{1}$$

and finally we have

$$\frac{\mathrm{LV}}{|\,u_h\,|_{1,1}}\leqslant\frac{Ch\,|\,u\,|_{1,1}+O(h^{N+1})}{|\,u\,|_{1,1}}\sim Ch. \tag{2}$$

Now, we define the indicator as $\dfrac{\mathrm{LV}}{|u_h|_{1,1}h}$.

Suppose the current element contains a discontinuity, the above error estimates are not held and an abrupt increase of LV can be observed due to the aliasing-driven instability. In practical uses, a problem dependent threshold value will be given, and beyond this value the current cell is indicated as a trouble cell.

3 Gegenbauer Reconstruction

A Gegenbauer reconstruction (GR) technique is used here to wipe off the oscillations, see more details in references [14-15]. For the given number of m and λ, the GR procedure is implemented in each intervals consists of the following two steps.

Step 1 Compute the coefficients of Gegenbauer expansion for $q(x)$, as

$$\hat{g}_k^{\lambda}=\frac{1}{h_k^{\lambda}}\int_{-1}^{1}(1-x^2)^{\lambda-\frac{1}{2}}q(x)C_k^{\lambda}(x)\mathrm{d}x. \tag{3}$$

Where $C_k^{\lambda}(x)$ are the Gegenbauer polynomials, and satisfy the recurrence relation

$$C_k^{\lambda}(x)=\frac{2(\lambda+k-1)}{k}xC_{k-1}^{\lambda}(x)-\frac{2\lambda+k-2}{k}C_{k-2}^{\lambda}(x), \tag{4}$$

and $0\leqslant k\leqslant m$. The first two Gegenbauer polynomials are given by $C_0^{\lambda}(x)=1$, $C_1^{\lambda}(x)=2\lambda x$, and the normalization constants are

$$h_k^{\lambda}(x)=\pi^{\frac{1}{2}}\frac{\Gamma(k+2\lambda)}{n!\Gamma(2\lambda)}\frac{\Gamma(\lambda+1/2)}{\Gamma(\lambda)(k+\lambda)}. \tag{5}$$

where $\Gamma(x)$ is Gamma function. The exact integration is available with the help of numerical integration method based on Gauss quadrature rule. To evaluate the values at the quadrature points, we take a different way from the original GR method in the spectral method. In the DG method, these values can be interpolated directly, while in the original version, they need to be recomputed from a global approximation of the whole domain.

Step 2　Construct the Gegenbauer series $q^G = \sum_{k=0}^{m} \hat{g}_k^{\lambda} C_k^{\lambda}(x)$. It is proved that the truncation and regularization errors of the reconstructed solution can be exponentially small for appropriate choice of λ and m. The choice suggested in references [14] is $\lambda = 0.2N_{\text{node}}$ and $m = 0.1N_{\text{node}}$, N_{node} is the total number of node in the global approximations.

4　Numerical Examples

4.1　Burgers Equation

Consider one dimensional Burgers equation $\frac{\mathrm{d}u}{\mathrm{d}t} + \frac{\mathrm{d}}{\mathrm{d}x}\left(\frac{u^2}{2}\right) = 0$, $u(x;0) = 0.5 + \sin(\pi x)$. Using a nodal DG method of the fifth order with a mesh of 100 nodal points to solve the above equation, we obtain the numerical solution at time $1.5/\pi$ with a discontinuity lying in the region $[1.2, 1.3]$, see Fig. 1. Nearby the discontinuity, the density oscillates acutely. The local variations after some post processing techniques computed according to the definition formula are drawn in Fig. 2. The variations below a given threshold value will be set to zero, and only the elements have relatively bigger values are retained and are marked as trouble cells. It is noted that a misjudged point in the smooth region after the discontinuity appears, and the mechanism is still unknown. Since the GR procedure is applied to ease the surges, the mismark is neglected. After implementing the GR procedure, the solution is recovered in Fig. 3. All oscillations are wiped off totally, and in smooth regions the reconstructed solution fits well to the exact solution. The points very near to the discontinuity have small discrepancies with respect to the exact solution.

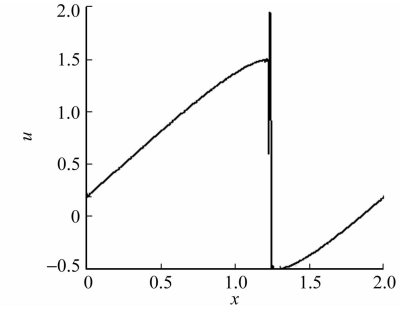

Fig. 1　Solution of Burgers equation

图 1　Burgers 方程数值解

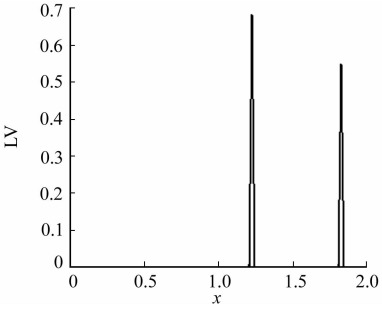

Fig. 2　Local variations of Burgers solution

图 2　Burgers 数值解的局部变差

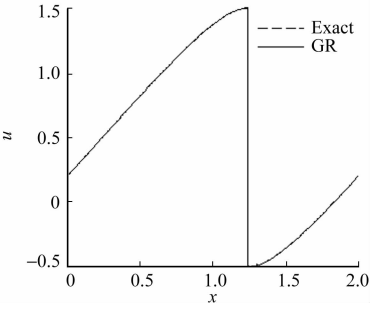

Fig. 3　GR solution for Burgers equation

图 3　Burgers 方程的重构解

4.2　Shock Tube Problem

We now test the indicator on nonlinear system of Euler equations. Consider the hyperbolic system with the conservative vector and flux of the following form

$$\boldsymbol{U} = (\rho, \rho u, E)^{\mathrm{T}}, \qquad \boldsymbol{F} = (\rho u, \rho u^2 + p, u(E+p))^{\mathrm{T}}. \tag{6}$$

Where ρ is density, u is velocity, E is total energy, p is pressure, and $E = p/(\gamma - 1) + \frac{1}{2}\rho u^2$ with $\gamma = 1.4$. In domain $\Omega = [-1, 1]$, the initial conditions are $(\rho, u, p) = \begin{cases} (1, 0, 1), & x \leqslant 0.5; \\ (0.125, 0, 0.1), & x > 0.5. \end{cases}$

A rough solution solved by the 5th order DG method with a 100 elements mesh is given in Fig. 4. The solution is obtained at $t = 2.0$. Obvious oscillations appear nearby the contact discontinuity and the shock, and even in both ends of the expansion region. The local variation indicators drawn in Fig. 5 suggest 4 positions to be marked. According the exact solution from the exact Riemann solver, the locations of discontinuities captured are precisely correct, which makes an excellent start for the next reconstructions. The GR solution in Fig. 6 shows an approving result except a moderate discrepancy

right before the shock. In fact, the region between the contact discontinuity and the shock is polluted so severely by the numerical oscillations that it is challenging for any of the reconstruction techniques to recover a satisfactory smoothness and accuracy.

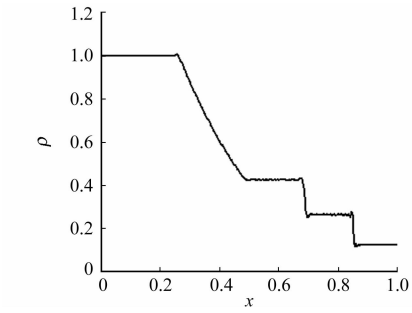

Fig. 4 Solution of shock tube problem

图 4 激波管问题数值解

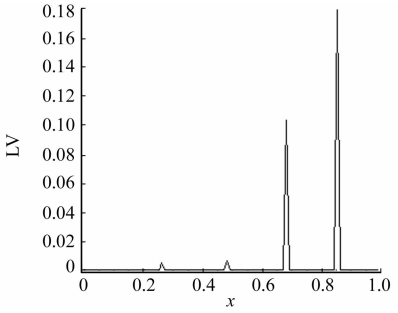

Fig. 5 Local variations of solution of shock tube problem

图 5 激波管问题解的局部变差

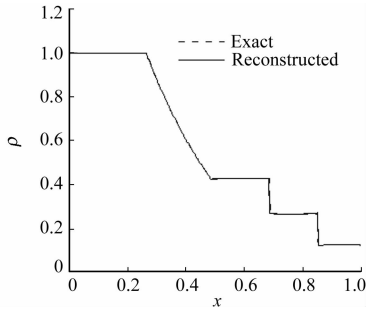

Fig. 6 GR solution for shock tube problem

图 6 激波管问题的重构解

4.3 Osher Shu Problem

We try another more complex example, the Osher Shu problem. This problem describes a Mach 3 shock interacts with a density wave. And its initial conditions are listed below

$$(\rho,u,p)=\begin{cases}(3.857\ 143,2.629\ 369,10.333\ 333), & x\leqslant -4,\\ (1+0.2\sin(5x),0,0.1), & x>-4.\end{cases} \tag{7}$$

The initial position of the shock is at $x=-4$ and moves toward the right direction immediately. The region right to the shock is a density wave with a sine shape distribution. The main characteristics of the Osher Shu problem are very strong discontinuities and the very fine structures in the smooth regions. Employing the fifth order accuracy DG method, a rough solution at $t=1.8$ is obtained based on a mesh of 400 elements. The result is shown in Fig. 7. Again, the result shows a wonderful simulation in the complex smooth regions but unwanted oscillations nearby the discontinuities. Since there has been no exact solution for this problem so far, the exact part is absent in the figure. Thanks to the local variation indicators, several discontinuities locations are captured in Fig. 8. Similar to the indicators of Burgers equation, some mismarks are detected as well as the discontinuities. A further survey suggests these mismarks are the points with extrema. This means our indicators based on the local variations confuse moderate discontinuities and extrema. How to distinguish them is our future work and the terms of derivatives would be considered. The reconstructed solution is in Fig. 9 and also shows reasonable effects.

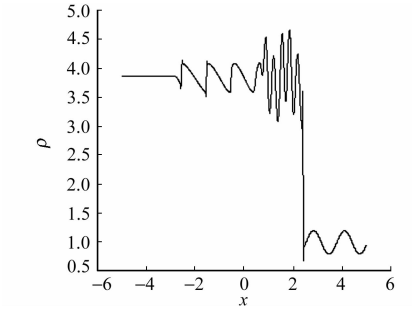

Fig. 7 Solution of Osher Shu problem

图 7 Osher Shu 问题的数值解

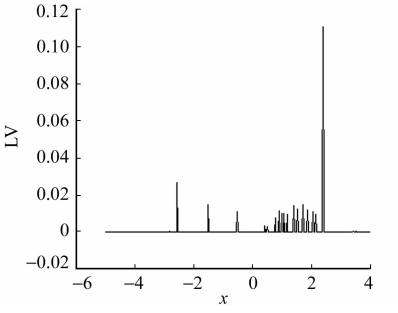

Fig. 8 Local variations of Osher Shu solution

图 8 Osher Shu 的局部变差

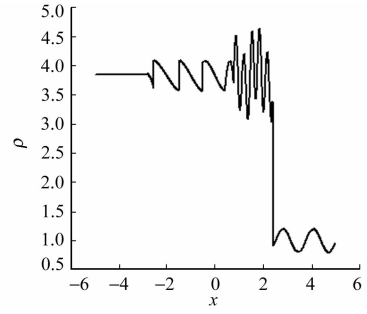

Fig. 9 GR solution of Osher Shu problem

图 9 Osher Shu 问题的重构解

5 Conclusions

A new discontinuity indicator based on local variation is presented for DG methods. The indicator

is elementally local and is very simple to implement. The bounded error evaluation makes a sound theory foundation for the application of the indicator. And applications to the typical numerical examples show a good performance of the indicator. Combined with the oscillation eliminating techniques, the DG method with new indicators is able to identify the discontinuities and suppress the oscillations effectively. Though the new indicator cannot distinguish an extremum and a discontinuity, but more efficient limiters like WENO limiters can alleviate the burden. More advanced indicators considering higher order derivatives will be constructed in our future work.

References:

[1] 王金平,庄清渠. 五阶常微分方程的 Petrov-Galerkin 谱元法[J]. 华侨大学学报(自然科学版),2017,38(3):435-440. DOI:10.11830/ISSN.1000-5013.201703027.

[2] 吴胜,庄清渠. 三阶微分方程的 Legendre-Petrov-Galerkin 谱元方法[J]. 华侨大学学报(自然科学版),2013,34(3):344-348. DOI:10.11830/ISSN.1000-5013.2013.03.0344.

[3] SHU Chiwang. TVB uniformly high-order schemes for conservation laws[J]. Mathematics of Computation,1987,179(49):105-121. DOI:10.1090/S0025-5718-1987-0890256-5.

[4] KRIVODONOVA L,XIN J,REMACLE J F,*et al*. Shock detection and limiting with discontinuous Galerkin methods for hyperbolic conservation laws[J]. Applied Numerical Mathematics,2004,48(3/4):323-338. DOI:10.1016/j.apnum.2003.11.002.

[5] 梁俊龙,张贵田,秦艳平. 基于高阶 WENO 格式的喷管动态特性仿真分析[J]. 火箭推进,2015,41(4):29-36. DOI:10.3969/j.issn.1672-9374.2015.04.005.

[6] LUO H,BAUM J D,LHNER R. On the computation of steady-state compressible flows using a discontinuous Galerkin method[J]. International Journal for Numerical Methods in Engineering,2008,73(5):597-623. DOI:10.1007/978-3-540-92779-2_4.

[7] 郝海兵,杨永,左岁寒. 间断探测器在间断 Galerkin 方法中的应用[J]. 航空计算技术,2011,41(1):14-18. DOI:10.3969/j.issn.1671-654X.2011.01.004.

[8] ZHONG Xinghui,SHU Chiwang. A simple weighted essentially nonoscillatory limiter for Runge-Kutta discontinuous Galerkin methods[J]. J Comput Phys,2013,232(1):397-415. DOI:10.1016/j.jcp.2012.08.028.

[9] ZHU Jun,ZHONG Xinghui,SHU Chiwang,*et al*. Runge-Kutta discontinuous Galerkin method using a new type of WENO limiters on unstructured meshes[J]. J Comput Phys,2013,248(2):200-220. DOI:10.1016/j.jcp.2013.04.012.

[10] 张来平,刘伟,贺立新,等. 一种新的间断侦测器及其在 DGM 中的应用[J]. 空气动力学学报,2011,29(4):401-406. DOI:10.3969/j.issn.0258-1825.2011.04.001.

[11] GOTTLIEB S,SHU Chiwang,TADMOR E. Strong stability preserving high-order time discretization methods[J]. SIAM Review,2001,43(1):89-112. DOI:10.1137/S003614450036757X.

[12] GOTTLIEB S. On high order strong stability preserving Runge-Kutta and multi step time discretizations[J]. J Sci Comput,2005,25(1/2):105-128. DOI:10.1007/s10915-004-4635-5.

[13] HESTHAVEN J S,WARBURTON T. Nodal discontinuous Galerkin methods algorithms, analysis and applications[M]. New York:Springer,2008.

[14] GOTTLIEB D,SHU Chiwang. On the Gibbs phenomenon Ⅳ: Recovering exponential accuracy in a subinterval from a Gegenbauer partial sum of a piecewise analytic function[J]. Math Comp,1995,64(211):1081-1095. DOI:10.1090/S0025-5718-1995-1284667-0.

[15] SHIZGAL B D,JUNG J H. Towards the resolution of the Gibbs phenomena[J]. J Comput Appl Math,2003,161:41-65. DOI:10.1016/S0377-0427(03)00500-4.

(责任编辑: 钱筠　　**英文审校:** 崔长彩)